NANO LETTERS

Letter

One-Dimensional Coupling of Gold Nanoparticle Plasmons in Self-Assembled Ring Superstructures

Wei-Shun Chang, Liane S. Slaughter, Bishnu P. Khanal, Pramit Manna, Eugene R. Zubarev, and Stephan Link

Nano Lett., **2009**, 9 (3), 1152-1157• DOI: 10.1021/nl803796d • Publication Date (Web): 04 February 2009

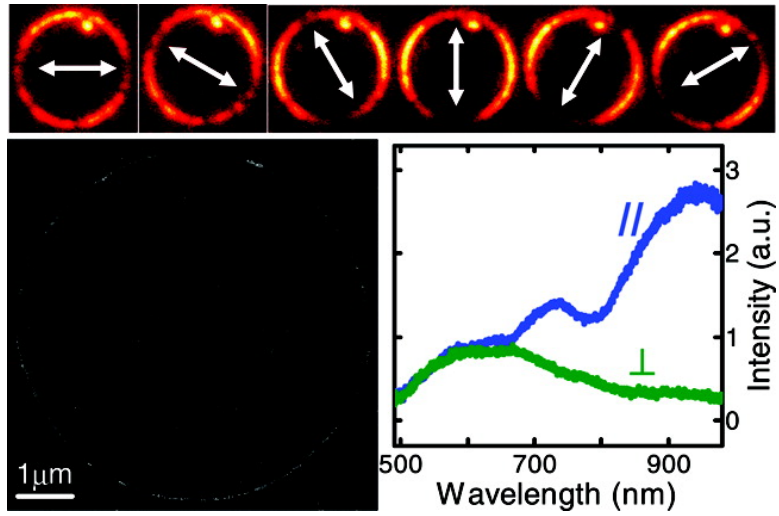

More About This Article

Additional resources and features associated with this article are available within the HTML version:

- Supporting Information
- Access to high resolution figures
- Links to articles and content related to this article
- Copyright permission to reproduce figures and/or text from this article

View the Full Text HTML

NANO LETTERS

2009
Vol. 9, No. 3
1152-1157

One-Dimensional Coupling of Gold Nanoparticle Plasmons in Self-Assembled Ring Superstructures

Wei-Shun Chang,[†,§] Liane S. Slaughter,[†,§] Bishnu P. Khanal,[†] Pramit Manna,[†] Eugene R. Zubarev,[†] and Stephan Link*[,†,‡]

Department of Chemistry, Department of Electrical and Computer Engineering, Rice University, Houston, Texas 77005

Received December 16, 2008; Revised Manuscript Received January 27, 2009

ABSTRACT

Plasmon coupling in ordered metal nanoparticle assemblies leads to tunable collective surface plasmon resonances that strongly depend on the interparticle distance. Here we report on the surface plasmon scattering of polystyrene-functionalized 40 nm gold nanoparticles self-assembled into close-packed rings. Using single particle dark-field scattering spectroscopy, we observed strong near-field coupling between neighboring nanoparticles, which results in red-shifted multipolar plasmon modes highly polarized along the ring circumference. Correlated optical spectroscopy and scanning electron microscopy of individual rings with different diameters revealed that the plasmon coupling is independent of ring curvature and mostly insensitive to the local nanoparticle arrangement. Our results further suggest that a one-dimensional gold nanoparticle assembly yields long-range collective plasmonic properties similar to those of metallic nanowires.

Changes in the size, shape, and dielectric environment provide an extraordinary degree of freedom for manipulating the localized surface plasmon oscillation frequency and lifetime in isolated metal particles.[1−3] Applications of the surface plasmon resonance in novel solid-state devices require the assembly of nanoparticles into ordered structures. When the interparticle distance becomes comparable to the wavelength of the interacting light, far-field radiative coupling[4−6] strongly modifies the plasmon resonance energy and width. In linear nanoparticle chains with the interparticle distance close to the single particle resonance wavelength, far-field interference causes a narrow plasmon mode polarized perpendicular to the nanoparticle chain to emerge, as observed for 100 nm × 30 nm silver disks.[4] Calculations using the coupled dipole approximation predict that the width of this plasmon resonance can be smaller than 1 nm with a refractive index sensing sensitivity, which is four times larger than that of the corresponding isolated nanoparticle.[7]

As the interparticle separation is decreased to distances equal or less than the nanoparticle diameter, near-field interactions become important and, in linear chains,[8−17] lead to a splitting of the plasmon resonance into two propagating plasmon modes polarized parallel and perpendicular to the major chain axis. Within the quasi-static point dipole approximation, the energy splitting, caused by a blueshift of the transverse and redshift of the longitudinal plasmon mode, is directly related to the plasmon propagation loss.[8] Propagation lengths as large as micrometers have been predicted for plasmon waveguides constructed from nanoparticles chains.[18,19] Using near-field scanning optical microscopy (NSOM) and fluorescence markers, energy transport by the coupled transverse mode over a distance of 500 nm has been confirmed in a linear chain of 90 nm × 30 nm silver nanorods with 50 nm gaps.[9] But even at small interparticle distances, far-field radiative coupling cannot be neglected and its effect must be considered in the design of novel plasmonic elements.[11−13,20] For example, phase retardation and interference in a linear chain of 110 nm × 50 nm silver nanodisks and center-to-center separations of 150 nm lead to the localization of different wavelengths at the opposite ends of the chain.[13]

The ability to produce arrays with homogeneous particle size and shape as well as regular interparticle separations using lithography techniques has provided invaluable insight into the far- and near-field interactions of surface plasmons in ordered metal nanoparticle structures.[5,6,9−11,13] The results obtained to date clearly demonstrate the tremendous potential of using metal nanoparticles in plasmonic devices to receive and transmit light. However, it is difficult to reproducibly fabricate gaps of only a few nanometers that result in even larger near-field coupling[15] using e-beam lithography. In self-assembled mesostructures of chemically prepared metal nanoparticles, the length and the grafting density of the

* To whom correspondence should be addressed. E-mail: slink@rice.edu.
† Department of Chemistry.
‡ Department of Electrical and Computer Engineering.
§ Authors contributed equally and appear in alphabetical order.

10.1021/nl803796d CCC: $40.75
Published on Web 02/04/2009

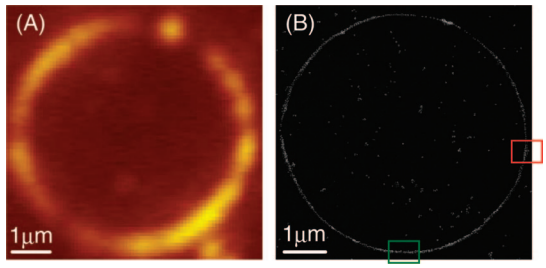

Figure 1. Correlated dark-field scattering (A) and SEM (B) images of a 6 μm diameter ring composed of polystyrene-functionalized 40 nm gold nanoparticles. Magnified views of the ring segments marked by the green and red rectangles in (B) are shown in Figure 2.

surface capping material determine the minimum interparticle distance. The redshift of the plasmon resonance due to near-field interactions has already been exploited for sensitive colorimetric detection of biomolecular recognitions events using DNA-functionalized gold nanoparticles.[21,22] For nanoparticle dimers, the distance-dependent plasmon coupling has been utilized in a plasmon ruler to measure the size of biopolymers in solution.[23,24] However, while the controlled assembly of chemically prepared nanoparticles into larger superstructures with an overall defined microscopic shape has attracted much interest,[25−36] only little is known about far- and near-field plasmon interactions in such assemblies.[37,38] An advantage of chemically synthesizing and assembling metallic nanoparticles is the relative low cost. Nevertheless, if plasmonic components made by chemical methods are supposed to rival those made by other fabrication techniques, it is necessary to first investigate and understand the plasmon coupling in chemically prepared nanoparticles assemblies, which typically provide favorably smaller, but inherently more irregular, interparticle separations.

Here we report on the plasmonic properties of chemically prepared 40 nm gold nanoparticles self-assembled into rings of different diameters. Covalent functionalization of the gold nanoparticles with polystyrene linear chains facilitated the breath figure assembly into ring structures with minimum interparticle distances of a few nanometers.[39] We chose rings of nanoparticles here because of their ease of preparation and the ability to easily vary the ring size. We observed redshifted multipolar plasmon modes, which are highly polarized parallel to the ring circumference and suggest long-range one-dimensional plasmon coupling along tens of nanoparticles. These higher order modes have not been observed previously in nanoparticle dimers with comparable interparticle distances or in linear chains with larger interparticle distances.[8−17] Combining scanning electron microscopy (SEM) with single particle dark-field scattering spectroscopy allowed us to correlate optical properties with the structural details of ring assemblies, which is essential for the systems that are inherently less ordered than nanoparticle arrays produced by e-beam lithography.

Correlated optical dark-field (Figure 1A) and structural SEM (Figure 1B) imaging of a ring with a diameter of 6 μm was accomplished by self-assembly of polystyrene-functionalized gold nanoparticles into ring structures on an

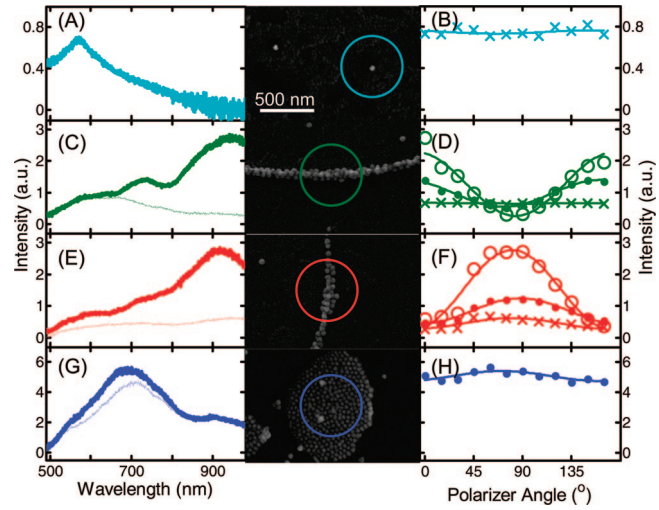

Figure 2. Dark-field scattering spectra of a single gold nanoparticle (A), the two ring segments highlighted in Figure 1B (C, E), and a nanoparticle aggregate (G). The thick (thin) lines show spectra recorded for scattered light polarized parallel (perpendicular) to the major axis of the nanoparticle assembly. The corresponding SEM images are given in the middle column with the size of the detection area highlighted by the colored circle. The right column shows the polarization dependence of the plasmon resonances for the single particle (B), the two ring segments (D, F), and the nanoparticle aggregate (H) measured at the three different resonance maxima. Note that the intensity scale on the right matches the one on the left.

ITO-coated glass slide.[39] The ring was composed of 40 ± 5 nm gold nanoparticles as determined by transmission electron microscopy. To assemble the nanoparticles into rings, cetyltrimethylammonium bromide stabilized nanoparticles[40,41] were covalently functionalized with mercaptophenol and esterified with carboxyl-terminated polystyrene chains (M_w = 10 000 g/mol),[39] rendering them highly soluble in nonpolar organic solvents. Allowing a drop of the nanoparticle chloroform solution to dry on the ITO-coated glass substrate, caused rings of various sizes to form at the interface between the organic solvent and water microdroplets that condensed from the air due to evaporative cooling of chloroform.[39] The interparticle distance varied along the assembled rings and depended on the concentration of the solution. Typical interparticle distances for the rings investigated here were 3 − 4 nm, in good agreement with the thickness of the polymer coating as determined by TEM.

Scattering images (Figure 1A) were collected on a home-built microscope employing a modified dark-field configuration in which the images were obtained by raster scanning the sample over a 50 μm pinhole located at the first image plane of the microscope. The pinhole allowed us to reject the out-of-focus excitation light and to acquire spectra from specific areas of the sample. Dark-field excitation was performed in a reflected light geometry using an inverted microscope with a tungsten lamp as the excitation source. The scattered light was imaged onto two avalanche photodiode detectors after passing through the pinhole and a polarizing beam splitter. To acquire scattering spectra, the light was redirected to a spectrometer equipped with a CCD camera.

Although the assembly of rings can be achieved with nanoparticles of any shape as long as they are functionalized with polystyrene,[39] we chose here to study rings composed of nanoparticles with almost spherical shape. Figure 2A shows the scattering spectrum of a single nanoparticle as confirmed by SEM. The insensitivity of the spectrum to the polarization of the scattered light and the presence of only a single plasmon maximum confirms the spherical shape of the nanoparticles. Figure 2B shows the intensity at the plasmon resonance maximum as a function of the angle of a polarizer placed in the detection path after the pinhole. The weak polarization dependence and the limited spectral dispersion of the scattering spectra for the unassembled isolated nanoparticles aided in unambiguous observation of coupled plasmon modes in the spectra of the rings as shown below.

Strong near-field interactions of the nanoparticle plasmons in the 6 μm self-assembled ring shown in Figure 1 are evident from the scattering spectra that were recorded along the ring circumference for quasi one-dimensional segments with dimensions of ~500−600 nm in length determined by the size of the pinhole. Figure 2C,E displays the scattering spectra polarized parallel (thick line) and perpendicular (thin line) to the ring circumference for the two segments marked in Figure 1B with magnified views given in the middle column of Figure 2. In comparison to the single nanoparticle scattering spectrum with only one plasmon resonance at 570 nm (Figure 2A), the spectra taken from nine ring segments show at least three distinct plasmon resonances within our spectral observation window, having average maxima at 935 $\pm$ 28, 735 $\pm$ 15, and 619 $\pm$ 24 nm.

The polarization dependence of the two most red-shifted plasmon modes in the ring scattering spectra reveals that the plasmon coupling preferentially occurs in a quasi one-dimensional direction along the ring circumference. In addition to the spectra shown in Figure 2C,E recorded with polarization horizontal and vertical with respect to the image plane, we also measured the scattering spectra as a function of polarizer angle. The intensities of the three plasmon resonances identified in Figure 2C,E are plotted versus polarizer angle in Figure 2D,F, respectively. An angle of zero corresponds here to horizontal polarization. In Figure 2D,F the longest wavelength coupled plasmon mode (open circles) reaches a maximum intensity when the polarization is parallel to the local alignment of the nanoparticles and a minimum intensity for the perpendicular polarization. As expected from the orthogonal orientation of the two ring segments, the intensities oscillate 90° out of phase with respect to each other. The polarization dependence of the longest wavelength scattering resonance can be fitted well to a $\cos^2(\theta)$ function (solid lines) consistent with a dipole or higher odd-order longitudinal plasmon oscillation. The large modulation depth of almost 90% indicates nearly complete longitudinal oscillation tangential to the ring circumference as was further confirmed by all polarized spectra taken at other positions.

Despite a slightly lower modulation depth of ~65%, the plasmon resonance at 735 $\pm$ 15 nm shows a similar polarization dependence as the lowest energy plasmon resonance (Figure 2D,F, solid circles), suggesting that it is also a coupled plasmon mode. In contrast, the scattered light intensity of the highest energy peak is almost completely unpolarized. Given the large resonance width, it is unlikely that this peak simply arises from the sum of the scattering spectra of the single nanoparticles within the detection area. We therefore assign the highest energy plasmon resonance to a superposition of a coupled transverse mode with a higher order longitudinal mode. A pure transverse mode is however not observed in any of the rings measured.

To examine the significance of the linear arrangement of nanoparticles in the ring and its effect on the plasmon coupling we also investigated a circularly shaped aggregate assembled from the same nanoparticles with a diameter of about 900 nm. The polarized scattering spectra are given in Figures 2G together with corresponding SEM image. The spectra in Figure 2G show a broad peak centered around 700 nm with a shoulder at 900 nm indicating that near-field interaction between the plasmons are also important in this close-packed nanoparticle assembly. However, the absence of a distinct polarization dependence of the scattering peaks (Figure 2H) for the circularly shaped aggregate in comparison to the ring corroborates our conclusion that a one-dimensional nanoparticle alignment results in a directional coupling of the localized surface plasmon. These measurements highlight the importance of the overall geometry of the assembled structure for the design of plasmonic components based on near-field interactions between nanoparticle plasmons.

To spatially visualize the coupled plasmon modes of the assembled ring, we performed polarization- and wavelength-selective dark-field microscopy by imaging the scattering intensity with filters inserted in the optical detection path and splitting the signal into orthogonal polarizations. Dark-field images of the same 6 μm ring shown in Figure 1 recorded at wavelengths of 550 $\pm$ 20 (Figure 3A,B) and 900 $\pm$ 20 nm (Figure 3C,D) confirm the presence of a coupled plasmon mode at 900 nm that is polarized along the ring circumference. These results differ from those reported for continuous nanorings with submicrometer diameters for which the lowest energy surface plasmon resonance originates from the coupling of dipolar modes at the inner and outer surfaces of the nanorings resulting in an opposite polarization dependence as observed here.[42,43]

Our results also differ from scattering spectra measured on 2 μm diameter rings of nanoparticles prepared by e-beam lithography.[44] Those rings consisted of 100 nm gold disks spaced 200 nm apart. The scattering spectra of the rings and the isolated disks were identical indicating weak or no near-field interactions as verified independently by Raman scattering experiments[44] and as expected for interparticle distances on the order of twice the particle diameter.[10,17,45] Instead, far-field interference due to phase shifts between the scattered light originating from different particles in these rings dominates the scattering images and leads to bright and dim ring segments for perpendicular and parallel

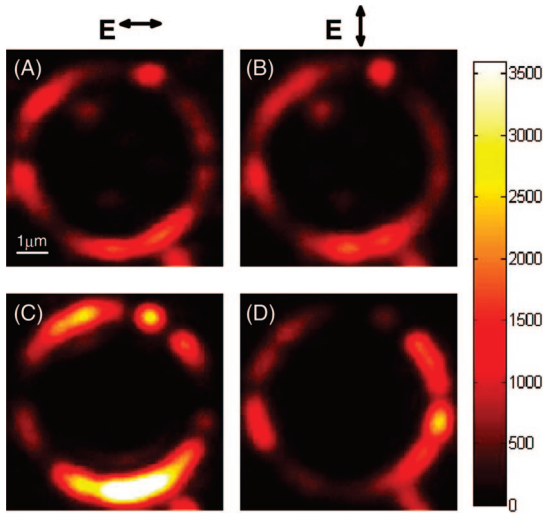

Figure 3. Polarization- and wavelength-selective dark-field microscopy of the 6 μm ring shown in Figure 1. (A, B) 550 $\pm$ 20 nm; (C, D) 900 $\pm$ 20 nm. The polarization of the scattered light is indicated by the arrows. A constant background has been subtracted from all images.

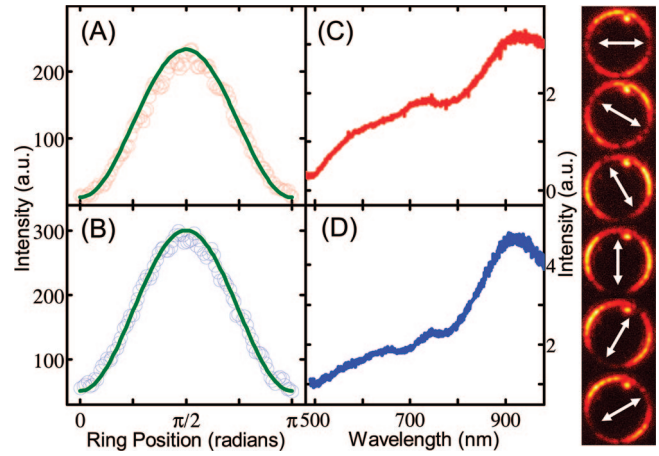

Figure 4. Dependence of the scattering intensity on the ring curvature (A, B) and spectral insensitivity of the coupled plasmon modes on the ring position and diameter (C, D). The scattering intensity at 900 $\pm$ 20 nm, obtained by taking images as a function of polarizer angle and averaging the intensity for all semicircles, is plotted as a function of relative ring position for a 6 μm (panel A) and 8 μm (panel B) diameter ring. Images of the 8 μm ring are shown on the right with the detected polarization axis given by the white arrows. The solid green lines are plots of $\sin^2(\theta)$ scaled to the experimental scattering intensity. Ensemble spectrum of the 6 μm ring (C) measured at nine different locations and scattering spectrum of the 8 μm ring (D) taken at a single location.

polarization of the incident light, respectively.[44] In contrast, far-field interactions most likely play only a minor role in the scattering images of the rings of nanoparticles studied here because far-field diffractive coupling occurs for polarization perpendicular to the nanoparticle chain[4,7,13,20] and requires long-range periodicity in the nanoparticle arrangement.[5]

Next nearest neighbor dipolar coupling has been reported to be small in linear nanoparticle chains,[10,18] consistent with the exponential distance dependence of near-field interactions in nanoparticle dimers.[15−17] Although multipole coupling becomes important for interparticle separation of a few nanometers,[15,16,46] nearest neighbor interactions are also expected to dominate in the rings assembled from 40 nm gold nanoparticles. This is confirmed in Figure 4, in which polarization-dependent images were analyzed for scattering intensity versus relative ring position at the longest wavelength resonance. The series of scattering images for an 8 μm ring included in Figure 4 gives a pictorial overview of this analysis, which involves averaging the intensity for all semicircles with the detected polarization axis (white arrows) determining 0 and π for each setting of the polarizer angle. The relative ring position intensities are overlain in Figure 4A,B with a $\sin^2(\theta)$ function scaled to the measured scattering intensity (green line). The excellent agreement between the experimental data and the expected $\sin^2(\theta)$ distribution demonstrates that for all positions along the ring circumference the scattering intensity originates from a dipole-like plasmon mode and is determined by the relative orientations of the light polarization and the nearest neighbor alignment. This relationship also implies that the intensity distribution should scale with the ring curvature, and this is indeed observed when comparing the analysis of the 6 μm diameter (Figure 4A) ring with a larger 8 μm diameter (Figure 4B) ring. Note that the intensity distribution as a function of absolute distance along the ring circumference is given by the angle given in Figure 4A,B multiplied by the ring radius, which then gives the dependence of the scattering intensity on the ring curvature.

Although larger interparticle gaps combined with thicker regions of the ring gave rise to variations in the scattering intensity (see Figures 1 and 3), analyzing the spectra taken along the 6 μm ring and comparing the spectra to the structural information obtained by SEM surprisingly indicates that the scattering spectra are mostly insensitive to the precise local arrangement of the nanoparticles. This can be seen from the magnified SEM images and the corresponding spectra shown in Figures 2, as well as by comparing the spectra with each other. The individual scattering spectra are in fact well described by the ensemble ring spectrum constructed from averaging nine individual spectra taken with polarization parallel to the local ring segment (Figure 4C). The insensitivity of the coupled plasmon resonances to "defects" in the nanoparticle arrangement suggests that, in addition to nearest neighbor coupling, long-range plasmon interactions over distances spanning many nanoparticles must also contribute to the spectral profile here.

Previous studies on linear nanoparticle chains[8−13] and nanoparticle dimers[14−17] showed a distinct energy splitting into transverse and longitudinal plasmon modes. However, this is not observed here. Instead, we assign the red-shifted coupled plasmon resonances of the ring to multipolar plasmon modes similar to those observed for long nanorods or nanowires.[47−52] The extinction spectra of colloidal gold nanorods[50] with diameters of 85 nm and aspect ratios greater than 4 as well as silver nanowires[51,52] prepared by electron e-beam lithography (85 nm wide, 25 nm high) show several multipolar plasmon resonances in addition to the transverse and longitudinal modes expected from smaller nanorods.[53] Theoretical studies have confirmed that the dipole and higher

odd-order multipole modes are polarized along the long axis, that the scattering intensity increases with decreasing order of the multipole, and that the highest energy resonance is composed of multipole longitudinal and transverse modes.[47,48] The ring spectra show all of these properties of such multipolar plasmon modes. Multipole plasmon resonances can be understood as standing waves excited in an extended metallic structure,[47,48,52] and a direct visualization of a standing plasmon wave has been accomplished using NSOM.[54]

Upon comparing the spectral features of the self-assembled ring with the plasmonic properties of nanowires, we therefore interpret the multiple plasmon resonances in the ring scattering spectra as a result of the nanoparticle assembly collectively behaving as a continuous elongated quasi one-dimensional nanostructure that supports multipolar plasmon modes. Assuming that a quasi linear segment of the close-packed nanoparticles resembles a nanorod and approximating the thickness of the 6 μm diameter ring to be 120 nm (i.e., 2−3 particles thick), we can estimate the equivalent nanorod length by assigning the two longitudinally polarized plasmon resonances at 935 ± 28 and 735 ± 15 nm to odd-order multipole modes l according to published results obtained from calculations using the discrete dipole approximation (DDA).[47] The best agreement between the measured scattering spectra of the ring and theory for 120 nm thick nanorods is achieved when the two lowest energy ring resonances correspond to either $l = 5$ and $l = 7$, equivalent to a nanorod length of 900 nm, or $l = 3$ and $l = 5$, equivalent to a nanorod length of 600 nm.[47] For this comparison, we used an average medium refractive index of ITO glass and air.[15] Further experiments covering an extended wavelength range are planned to verify this interpretation and allow for an explicit mode assignment.

Interestingly, the scattering spectrum is not only insensitive to the ring position, but we also find that the spectral features of the 8 μm ring (Figure 4D) are very similar to those of the smaller 6 μm ring (Figure 4C), suggesting that a standing plasmon wave would be delocalized over a comparable distance despite the change in ring curvature and a different local ordering of the nanoparticles. It is not yet clear if an intrinsic limit is reached here as observed for a linear chain of 50 nm gold nanoparticles with a center-to-center separation of 75 nm prepared by e-beam lithography.[8] For the latter system, the magnitude of the energy splitting between the transverse and longitudinal plasmon modes saturates for 7 nanoparticles, agreeing with calculations predicting that the infinite chain limit is reached for 10 particles.[55,56]

In summary, using correlated SEM and dark-field scattering spectroscopy we have observed strong near-field plasmon coupling in a self-assembled ring of gold nanoparticles. The short interparticle distances, limited only by the covalently attached polystyrene chains, most likely facilitate the near-field interactions. We found that the geometry of the assembly is very important as quasi one-dimensional coupling occurred evenly along the ring circumference but was independent of the ring curvature. The spatially resolved scattering spectra revealed the presence of two additional plasmon bands that are red shifted from the single nanoparticle resonance and are polarized parallel to the local ring segment. Such additional multipolar modes have not been observed previously in linear chains made by e-beam lithography mostly likely because of larger interparticle separations. The spectral features of the rings are similar to those observed in long nanorods and nanowires. Comparing these features to DDA calculations on nanorods led us therefore to assign these spectral features to higher odd-order multipole plasmon modes, suggesting that the nanoparticle plasmons couple in such a way as to behave together as a one-dimensional nanostructure that is ∼20 times larger than the individual particles. Importantly, the persistence of the spectral features at almost all locations around the rings accentuates the robustness of plasmon coupling and its ability to tolerate defects within an assembly of nanoparticles. These results are important because they suggest that for small interparticle distances nanoparticle assemblies can behave similarly to continuous plasmonic structures. Hence, this presents a promising first step toward characterizing and manipulating plasmon coupling in chemically assembled one-dimensional structures and is central to realizing functional plasmonic components such as antennae and waveguides constructed from nanoparticle building blocks using bottom-up design strategies.

Acknowledgment. S.L. thanks the Robert A. Welch Foundation (Grant C-1664) and 3M for a Nontenured Faculty Grant. E.R.Z. acknowledges the financial support by NSF (DMR-0547399 and CBET-0506832), Robert A. Welch Foundation (C-1703), and Alfred P. Sloan Foundation. L.S.S. thanks the NSF IGERT Nanophotonics fellowship program. W.S.C. acknowledges support from the Richard E. Smalley Institute for a Peter and Ruth Nicholas fellowship. We would also like to thank Naomi Halas and Peter Nordlander for helpful discussions.

Supporting Information Available: Sample preparation and a description of the optical setup. This material is available free of charge via the Internet at http://pubs.acs.org.

References

(1) Kreibig, U.; Vollmer, M. *Optical Properties of Metal Clusters*; Springer: Berlin, 1995.
(2) Lal, S.; Link, S.; Halas, N. J. *Nat. Photonics* **2007**, *1*, 641.
(3) Kelly, K. L.; Coronado, E.; Zhao, L. L.; Schatz, G. C. *J. Phys. Chem. B* **2003**, *107*, 668.
(4) Hicks, E. M.; Zou, S.; Schatz, G. C.; Spears, K. G.; Van Duyne, R. P.; Gunnarsson, L.; Rindzevicius, T.; Kasemo, B.; Kall, M. *Nano Lett.* **2005**, *5*, 1065.
(5) Lamprecht, B.; Schider, G.; Lechner, R. T.; Ditlbacher, H.; Krenn, J. R.; Leitner, A.; Aussenegg, F. R. *Phys. Rev. Lett.* **2000**, *84*, 4721.
(6) Haynes, C. L.; McFarland, A. D.; Zhao, L.; Van Duyne, R. P.; Schatz, G. C.; Gunnarsson, L.; Prikulis, J.; Kasemo, B.; Käll, M. *J. Phys. Chem. B* **2003**, *107*, 7337.
(7) Zou, S.; Schatz, G. C. *J. Chem. Phys.* **2004**, *121*, 12606.
(8) Maier, S. A.; Kik, P. G.; Atwater, H. A. *Appl. Phys. Lett.* **2002**, *81*, 1714.
(9) Maier, S. A.; Kik, P. G.; Atwater, H. A.; Meltzer, S.; Harel, E.; Koel, B. E.; Requicha, A. A. G. *Nat. Mater.* **2003**, *2*, 229.
(10) Wei, Q.-H.; Su, K.-H.; Durant, S.; Zhang, X. *Nano Lett.* **2004**, *4*, 1067.
(11) Salerno, M.; Krenn, J. R.; Hohenau, A.; Ditlbacher, H.; Schider, G.; Leitner, A.; Aussenegg, F. R. *Opt. Commun.* **2005**, *248*, 543.
(12) Koenderink, A. F.; Rene de, W.; Jord, C. P.; Albert, P. *Phys. Rev. B* **2007**, *76*, 201403.

(13) deWaele, R.; Koenderink, A. F.; Polman, A. *Nano Lett.* **2007**, *7*, 2004.
(14) Rechberger, W.; Hohenau, A.; Leitner, A.; Krenn, J. R.; Lamprecht, B.; Aussenegg, F. R. *Opt. Commun.* **2003**, *220*, 137.
(15) Gunnarsson, L.; Rindzevicius, T.; Prikulis, J.; Kasemo, B.; Kall, M.; Zou, S.; Schatz, G. C. *J. Phys. Chem. B* **2005**, *109*, 1079.
(16) Jain, P. K.; Huang, W.; El-Sayed, M. A. *Nano Lett.* **2007**, *7*, 2080.
(17) Su, K.-H.; Wei, Q.-H.; Zhang, X.; Mock, J. J.; Smith, D. R.; Schultz, S. *Nano Lett.* **2003**, *3*, 1087.
(18) Brongersma, M. L.; Hartman, J. W.; Atwater, H. A. *Phys. Rev. B* **2000**, *62*, R16356.
(19) Quinten, M.; Leitner, A.; Krenn, J. R.; Aussenegg, F. R. *Opt. Lett.* **1998**, *23*, 1331.
(20) Hernandez, J. V.; Noordam, L. D.; Robicheaux, F. *J. Phys. Chem. B* **2005**, *109*, 15808.
(21) Elghanian, R.; Storhoff, J. J.; Mucic, R. C.; Letsinger, R. L.; Mirkin, C. A. *Science* **1997**, *277*, 1078.
(22) Alivisatos, A. P.; Johnsson, K. P.; Peng, X.; Wilson, T. E.; Loweth, C. J.; Bruchez, M. P., Jr.; Schultz, P. G. *Nature* **1996**, *382*, 609.
(23) Reinhard, B. M.; Siu, M.; Agarwal, H.; Alivisatos, A. P.; Liphardt, J. *Nano Lett.* **2005**, *5*, 2246.
(24) Soennichsen, C.; Reinhard, B. M.; Liphardt, J.; Alivisatos, A. P. *Nat. Biotechnol.* **2005**, *23*, 741.
(25) Boal, A. K.; Ilhan, F.; DeRouchey, J. E.; Thurn-Albrecht, T.; Russell, T. P.; Rotello, V. M. *Nature* **2000**, *404*, 746.
(26) Bunz, U. H. F. *Adv. Mater.* **2006**, *18*, 973.
(27) DeVries, G. A.; Brunnbauer, M.; Hu, Y.; Jackson, A. M.; Long, B.; Neltner, B. T.; Uzun, O.; Wunsch, B. H.; Stellacci, F. *Science* **2007**, *315*, 358.
(28) Pileni, M. P. *J. Phys. Chem. B* **2001**, *105*, 3358.
(29) Tang, Z.; Kotov, N. A. *Adv. Mater.* **2005**, *17*, 951.
(30) Xu, J.; Xia, J.; Lin, Z. *Angew. Chem., Int. Ed.* **2007**, *46*, 1860.
(31) Lin, S.; Li, M.; Dujardin, E.; Girard, C.; Mann, S. *Adv. Mater.* **2005**, *17*, 2553.
(32) Sardar, R.; Shumaker-Parry, J. S. *Nano Lett.* **2008**, *8*, 731.
(33) Nie, Z.; Fava, D.; Kumacheva, E.; Zou, S.; Walker, G. C.; Rubinstein, M. *Nat. Mater.* **2007**, *6*, 609.
(34) Thomas, K. G.; Barazzouk, S.; Ipe, B. I.; Joseph, S. T. S. J.; Kamat, P. V. *J. Phys. Chem. B* **2004**, *108*, 13066.
(35) Ohara, P. C.; Heath, J. R.; Gelbart, W. M. *Angew. Chem., Int. Ed.* **1997**, *36*, 1078.
(36) Yosef, G.; Rabani, E. *J. Phys. Chem. B* **2006**, *110*, 20965.
(37) Lee, J.; Hasan, W.; Lee, M. H.; Odom, T. W. *Adv. Mater.* **2007**, *19*, 4387.
(38) Ramakrishna, G.; Dai, Q.; Zou, J.; Huo, Q.; Goodson, T., III *J. Am. Chem. Soc.* **2007**, *129*, 1848.
(39) Khanal, B. P.; Zubarev, E. R. *Angew. Chem., Int. Ed.* **2007**, *46*, 2195.
(40) Sau, T. K.; Murphy, C. J. *J. Am. Chem. Soc.* **2004**, *126*, 8648.
(41) Sau, T. K.; Murphy, C. J. *Langmuir* **2004**, *20*, 6414.
(42) Aizpurua, J.; Hanarp, P.; Sutherland, D. S.; Käll, M.; Bryant, G. W.; de Abajo, F. J. G. *Phys. Rev. Lett.* **2003**, *90*, 057401.
(43) Hao, F.; Larsson, E. M.; Ali, T. A.; Sutherland, D. S.; Nordlander, P. *Chem. Phys. Lett.* **2008**, *458*, 262.
(44) Laurent, G.; Felidj, N.; Grand, J.; Aubard, J.; Levi, G.; Hohenau, A.; Aussenegg, F. R.; Krenn, J. R. *Phys. Rev. B* **2006**, *73*, 245417.
(45) Maier, S. A.; Brongersma, M. L.; Kik, P. G.; Atwater, H. A. *Phys. Rev. B* **2002**, *65*, 193408.
(46) Lassiter, J. B.; Aizpurua, J.; Hernandez, L. I.; Brandl, D. W.; Romero, I.; Lal, S.; Hafner, J. H.; Nordlander, P.; Halas, N. J. *Nano Lett.* **2008**, *8*, 1212.
(47) Encina, E. R.; Coronado, E. A. *J. Phys. Chem. C* **2007**, *111*, 16796.
(48) Khlebtsov, B. N.; Khlebtsov, N. G. *J. Phys. Chem. C* **2007**, *111*, 11516.
(49) Bryant, G. W.; de Abajo, F. J. G.; Aizpurua, J. *Nano Lett.* **2008**, *8*, 631.
(50) Payne, E. K.; Shuford, K. L.; Park, S.; Schatz, G. C.; Mirkin, C. A. *J. Phys. Chem. B* **2006**, *110*, 2150.
(51) Krenn, J. R.; Schider, G.; Rechberger, W.; Lamprecht, B.; Leitner, A.; Aussenegg, F. R.; Weeber, J. C. *Appl. Phys. Lett.* **2000**, *77*, 3379.
(52) Schider, G.; Krenn, J. R.; Hohenau, A.; Ditlbacher, H.; Leitner, A.; Aussenegg, F. R.; Schaich, W. L.; Puscasu, I.; Monacelli, B.; Boreman, G. *Phys. Rev. B* **2003**, *68*, 155427.
(53) Link, S.; El-Sayed, M. A. *J. Phys. Chem. B* **1999**, *103*, 8410.
(54) Okamoto, H.; Imura, K. *J. Mater. Chem.* **2006**, *16*, 3920.
(55) Citrin, D. S. *Nano Lett.* **2005**, *5*, 985.
(56) Quinten, M.; Kreibig, U. *Appl. Opt.* **1993**, *32*, 6173.

NL803796D